Redox Biology 47 (2021) 102154

Contents lists available at ScienceDirect

Redox Biology

journal homepage: www.elsevier.com/locate/redox

Selenoprotein K deficiency-induced apoptosis: A role for calpain and the ERS pathway☆

Shi-Zheng Jia [a,b], Xin-Wen Xu [a], Zhong-Hao Zhang [a,c], Chen Chen [a], Yu-Bin Chen [a], Shao-Ling Huang [a], Qiong Liu [a,b], Peter R. Hoffmann [d,**], Guo-Li Song [a,c,e,*]

[a] Shenzhen Key Laboratory of Marine Bioresources and Ecology, College of Life Sciences and Oceanography, Shenzhen University, Shenzhen, China
[b] Key Laboratory of Optoelectronic Devices and Systems of Ministry of Education and Guangdong Province, College of Optoelectronic Engineering, Shenzhen University, Shenzhen, China
[c] Shenzhen Bay Laboratory, Shenzhen, China
[d] Department of Cell and Molecular Biology, John A. Burns School of Medicine, University of Hawaii, Honolulu, HI, USA
[e] Shenzhen-Hong Kong Institute of Brain Science-Shenzhen Fundamental Research Institutions, Shenzhen, China

ARTICLE INFO

Keywords:
SELENOK
Calpain
Endoplasmic reticulum stress
Neuronal apoptosis

ABSTRACT

Selenoprotein K (SELENOK), an endoplasmic reticulum (ER) resident protein, is regulated by dietary selenium and expressed at a relatively high level in neurons. SELENOK has been shown to participate in oxidation resistance, calcium (Ca^{2+}) flux regulation, and the ER-associated degradation (ERAD) pathway in immune cells. However, its role in neurons has not been elucidated. Here, we demonstrated that SELENOK gene knockout markedly enhanced ER stress (ERS) and increased apoptosis in neurons. SELENOK gene knockout elicited intracellular Ca^{2+} flux and activated the *m*-calpain/caspase-12 cascade, thus inducing neuronal apoptosis both in vivo and in vitro. In addition, SELENOK knockout significantly reduced cognitive ability and increased anxiety in 7-month-old mice. Our findings reveal an unexpected role of SELENOK in regulating ERS-induced neuronal apoptosis.

1. Introduction

Selenium is an essential micronutrient that exhibits protective effects against oxidative stress in cells [1,2]. Selenium deficiency also leads to significant decreases in Ca^{2+}-ATPase activity, Ca^{2+} uptake capacity and Ca^{2+} uptake rate in cardiac sarcoplasmic reticulum isolated from rats [3]. Increased dietary selenium intake enhances Ca^{2+} flux and downstream cellular signaling in $CD4^{+}$ T cells, which dramatically affects their activation, proliferation, and differentiation [4]. Previous studies have shown that cognitive decline in humans is associated with a reduction in plasma selenium levels. Moreover, the brain retains more selenium than other tissues in a state of selenium deficiency [5], suggesting the indispensable role of selenium in the brain or neurons.

The biological role of selenium is exerted mostly through its incorporation into selenoproteins as the amino acid selenocysteine (Sec) [6,7]. Selenoprotein K (SELENOK) is a single-pass transmembrane protein that resides in the endoplasmic reticulum (ER) membrane [8]. SELENOK contains a cytosolic domain that includes a Sec residue located near the C-terminus. It is widely expressed in many tissues [9] and at particularly high levels in four brain regions [10]. Previous studies suggest that SELENOK can bind to ER-associated degradation (ERAD) components (p97, ATPase, Derlins, and SELENOS) [11]. The ERAD system is a quality control mechanism responsible for the degradation of misfolded proteins that inhibits their accumulation in the ER [12]. The accumulation of misfolded proteins in the ER triggers an adaptive ER stress (ERS) response termed the unfolded protein response (UPR) [13]. SELENOK is also required for palmitoylation of the Ca^{2+} channel protein inositol-1,4,5-triphosphate receptor (IP3R) in the ER

☆ This work was supported by Shenzhen Fundamental Research Program (No. JCYJ20200109105836705), Guangdong Natural Science Foundation for Major Cultivation Project (2018B030336001), National Natural Sciences Foundation of China (Nos. 31800681), Shenzhen-Hong Kong Institute of Brain Science-Shenzhen Fundamental Research Institutions (No. 2019SHIBS0003), NIAID/NIH grant R01AI089999.

* Corresponding author. Shenzhen Key Laboratory of Marine Bioresources and Ecology, College of Life Sciences and Oceanography, Shenzhen University, Shenzhen, China.
** Corresponding author.
E-mail addresses: peterrh@hawaii.edu (P.R. Hoffmann), lilys@szu.edu.cn (G.-L. Song).

https://doi.org/10.1016/j.redox.2021.102154
Received 23 August 2021; Received in revised form 26 September 2021; Accepted 27 September 2021
Available online 29 September 2021

membrane. Without this posttranslational modification, the function of IP3R is impaired [14], which can lead to deficiencies in calcium flux (Ca^{2+}) in the immune system [15]. IP3R also controls ER-mitochondria interactions, which are essential for efficient Ca^{2+} transfer, through the formation of the IP3R-Grp75-VDAC complex [16,17]. SELENOK knockout mice exhibit deficiencies in Ca^{2+} flux in immune cells [18]. Therefore, SELENOK plays essential roles in modulating ERS and Ca^{2+} homeostasis in immune cells. However, whether SELENOK plays a similar role in neurons and loss-of-function effects on neurons remain unclear.

In this study, we found that SELENOK gene knockout induced enhanced intracellular reactive oxygen species (ROS) production and cellular apoptosis in Neuro-2a (N2a) mouse neuroblastoma cells. Furthermore, SELENOK knockout increased neuronal apoptosis and intracellular Ca^{2+} concentrations in mice by activating the *m*-calpain/caspase-12 cascade, which led to impairment of cognitive ability in mice.

2. Materials and methods

2.1. Mice

SELENOK$^{-/-}$ mice generated on the C57BL/6 J background were generous gifts from the University of Hawaii. In this study, 7-month-old C57BL/6 J mice (n = 17; 8 males and 9 females) and SELENOK$^{-/-}$ mice (n = 17; 8 males and 9 females) were housed in individual ventilated cages (n = 3–4) assigned by group under a room temperature at 22 ± 2 °C under a 12 h alternating light/dark cycle with free access to food and water. The body weight of each mouse was recorded every 2 wks.

2.2. Western blot analysis

The mice were sacrificed after the behavioral tests. The brains were isolated and weighed. Then cortical and hippocampal tissues were dissected from the right hemibrain. The samples were homogenized in 8 vol of Tris-buffered saline (TBS) supplemented with a protease inhibitor mixture and phosphatase inhibitors (Roche, Basle Switzerland) and centrifuged at 12,000×*g* for 0.5 h at 4 °C. Then, the supernatant was collected, and the protein concentration of each sample was determined using the bicinchoninic acid assay (Sigma-Aldrich). Protein samples (10 μg) were separated by 8–12% SDS-polyacrylamide gel electrophoresis (SDS-PAGE) and transferred onto 0.45-μm polyvinylidene difluoride membranes (Millipore, Massachusetts, USA), the membranes were incubated overnight at 4 °C with primary antibodies recognizing tubulin (ab7291, from Abcam); or BIP(from Cell Signaling Technologies 3183), CHOP(from Cell Signaling Technologies 5554), activating transcription factor 6 (ATF6) (from Cell Signaling Technologies 65880), Calpain2 (from Cell Signaling Technologies 2539), and Caspase12, (from Cell Signaling Technologies 2202); Caspase3 from Cell Signaling Technologies 9661), or β-actin(from Proteintech 66009), GAPDH(from Proteintech 10494)., and then horseradish peroxidase-conjugated secondary antibodies (anti-rabbit and anti-mouse, NeoBioscience) were added for 1 h at 37 °C. The bands were visualized with an electroluminescence kit and scanned for densitometric analysis using an imaging system (Image Station 4000 M; Kodak) and Quantity One software (Bio-Rad). β-Actin, tubulin and GAPDH were used as loading controls.

2.3. Culturing of N2a and SELENOK$^{-/-}$ N2a cells

Mouse neuroblastoma N2a cells were purchased from ATCC, and the SELENOK gene was knocked out using the Integrated DNA Technology approach mediated by CRISPR-Cas9 as previously described (PMID 29568366). Two SELENOK$^{-/-}$ clonally derived cell lines named C13 and C15 were obtained and cultured in Opti-MEM/DMEM (1:1, v/v) supplemented with 6% fetal bovine serum, 100 mg/mL streptomycin and 100 U/mL penicillin at 37 °C in a humidified 5% CO2/95% air incubator.

2.4. Cell treatment

N2a and SELENOK$^{-/-}$ N2a cells were plated in a 6-well plate at a concentration of 10^5 cells per well. The levels of markers of ERS (BIP, CHOP, and ATF6) and apoptosis (Calpain2, Caspase12, and Caspase3) were measured by Western blot analysis. To verify the effects of SELENOK knock-out on ERS, ROS and calpain activity, the cells were also treated with specific ERS inducer or inhibitor, ROS inhibitor, and Calpain inhibitor respectively for 24 h. The following drugs were used: ERS inducer tunicamycin (TM, 11 μg/mL), ERS inhibitor salubrinal (30 μmol/mL) and sodium phenylbutyrate (4-PBA, 100 μmol/mL), ROS inhibitor Acetylcysteine (25 μmol/mL), and calpain inhibitor Calpeptin (2.5 μmol/mL).

2.5. Intracellular ROS level detection

Intracellular ROS levels were measured using a Reactive Oxygen Species Assay Kit (Beyotime S0033S). ROS can oxidize nonfluorescent DCFH-DA to fluorescent DCF; thus, fluorescence intensity was used to reflect intracellular ROS levels. N2a and SELENOK$^{-/-}$ N2a cells were washed twice with PBS, then 1 mL prepared medium comprised of 10 μmol/L DCFH-DA was added, and the cells were cultured for 20 min at 37 °C in the dark. The cells were then harvested, washed with PBS, resuspended in 500 μL PBS, and analyzed by flow cytometry.

2.6. Intracellular Ca^{2+} level assay by flow cytometry

Intracellular Ca^{2+} levels in N2a and SELENOK$^{-/-}$ N2a cells were measured by flow cytometry after labeling with Fluo-3/AM. Fluor-3 emits stronger fluorescence when it binds free Ca^{2+}. The cultured N2a and SELENOK$^{-/-}$ N2a cells were digested with 0.25% trypsin, collected, and then incubated with 5 μM Fluo-3/AM (Solarbio F8840) for 20 min at 37 °C. The cells were washed twice with HBSS, resuspended in 500 μL PBS, and immediately analyzed by flow cytometry at an excitation wavelength of 488 nm.

2.7. Assessment of cell apoptosis by flow cytometry

Cultured SELENOK$^{-/-}$ cells were collected, washed twice with medium without serum and antibiotics and twice with PBS, and then resuspended in 300 μL binding buffer. The cells were cultured with Annexin V-FITC solution for 15 min in the dark. After that, 3 μL propidium iodide (PI) solution was added, and the cells were cultured for 5 min. Finally, 200 μL binding buffer was added, and the cells were analyzed immediately by flow cytometry.

2.8. Measurement of the calpain activity by sandwich ELISA

Cultured N2a and SELENOK$^{-/-}$ N2a cells were collected and diluted with PBS (pH 7.2–7.4) to a concentration of 10^6 cells/mL. The cells were ruptured by repeated freezing and thawing to induce the release of intracellular components and centrifuged at 2500 rpm for 20 min. The supernatant was collected, and the calpain activity was measured with a Calpain ELISA Kit (MLbio, m1037795) according to the manufacturer's protocol.

2.9. Behavioral tests

The cognitive abilities of SELENOK$^{-/-}$ mice were evaluated when the mice were 7-months-old. All mice were subjected to a series of behavioral tests, including the Morris water maze, fear conditioning test, open field test and elevated plus-maze, with at least 24 h of rest between testing sessions.

2.10. Morris water maze

The Morris water maze, a classic test that evaluates spatial learning and memory, is widely used to assess the cognitive abilities of mice. The experiment was performed according to a previously published protocol [19].

2.11. Fear conditioning

The fear conditioning test consisted of two sessions: the training session and testing session. On the first training day, the mice were placed in a fear box for 2 min and then subjected to a tone (A: 80 Db, 30 s) and an electrical shock (B: 0.35 mA, 2 s) 1 s before the end of the tone. This A-B pairing was repeated four times. Twenty-four hours after the training, the mice were returned to the original training box for a 2 min context test session in which no tones or shocks were administered. An altered context test and conditional stimulus test were performed for 1 h of the correlation test. The fear box was modified as follows: the grid was replaced with smooth plastic. a colored plastic plate was placed along the diagonal of the box to make the rectangular box triangular, and olfactory cues were changed, such as by putting a cup of lemon juice on one side of the box. The mice were placed back into the fear chamber and recorded for 180 s, and then an auditory stimulus was delivered, and the mice were recorded for another 180 s. The freezing time of each mouse was determined. The floor of the chamber was cleaned with 75% ethanol solution between tests to prevent the spread of olfactory cues.

2.12. Open field test

The anxiety-related behaviors of 7-month-old SELENOK$^{-/-}$ mice were evaluated by the open field test. Briefly, the apparatus consisted of a white square box (70 cm long and 50 cm high) and a data acquisition system. The movement of each mouse was monitored by a camera mounted on the ceiling directly above the open field box. In each test, the mice were allowed to explore the box for 3 min, and the rearing time and exploring time were each recorded. The floor of the box was cleaned with 75% ethanol solution between tests to prevent the spread of olfactory cues.

2.13. Elevated plus-maze

The elevated plus-maze consisted of two open arms and two closed (wall-sheltered) arms. The test relies on an animal's natural inclination to stay in enclosed spaces and their unconditioned fear of open spaces and heights. In each test, the mice were allowed to explore the maze for 3 min. The movement of each mouse was monitored by a camera mounted on the ceiling above the elevated plus-maze, and the time spent in the closed arms (s), time spent in the open arms (s), and number of open-arm entries were recorded to evaluate anxiety.

2.14. Statistical analysis

The data were analyzed by GraphPad Prism software. All data were expressed as the mean ± SEM. Differences were considered significant at $p < 0.05$. Repeated-measured analysis of variance (ANOVA) was used to analyze the behavioral data. ANOVA or *t*-test was used to analyze the immunoblot data.

3. Results

3.1. SELENOK deficiency increases intracellular ROS levels in N2a cells

The expression levels of SELENOK were measured by Western blot analysis (Figs. S1A, C, D) and a very low level of SELENOK expression (a more than 91% decrease) was observed in SELENOK$^{-/-}$ (C13 and C15) N2a cells and in SELENOK$^{-/-}$mice. Besides, the brain weight of seven-month-old SELENOK$^{-/-}$ mice of significantly decreased comparing to that of WT mice (Fig. S2). SELENOK has been reported to have antioxidant properties. ROS levels were significantly increased in both SELENOK$^{-/-}$ (C13 and C15) N2a cells compared to wild-type (WT)N2a cells (Fig. 1A). These results confirmed that the SELENOK gene was effectively knocked out and that SELENOK knockout resulted in an increase in intracellular ROS levels in N2a cells.

3.2. SELENOK deficiency induces ERS and increases the intracellular free Ca^{2+} level

SELENOK has been reported to be involved in the regulation of ER homeostasis [11]. Silencing of the SELENOK gene by RNA interference significantly aggravates HepG2 cell apoptosis induced by ER stressors [20]. Therefore, we assessed the expression levels of ERS marker proteins. The levels of ATF6, BIP, and CHOP were all significantly increased in SELENOK$^{-/-}$ (C13 and C15) N2a cells compared with N2a(WT) cells (Fig. 1C and D). In addition, the levels of CHOP, ATF6 significantly increased in the cortical and hippocampal regions in 7-month-old SELENOK$^{-/-}$ mice (Fig. 1E–H). The ER is the major storage site for intracellular Ca^{2+} in cells. Significantly higher intracellular free Ca^{2+} levels were also observed in SELENOK$^{-/-}$ (C13 and C15) N2a cells compared with N2a(WT) cells (Fig. 1B).

3.3. SELENOK deficiency promoted ERS-induced N2a cells apoptosis

Severe and prolonged ERS can lead to cell apoptosis [21], which involves activation of the caspase-12 signaling pathway [22]. Therefore, we first assessed cell apoptosis by flow cytometry. The results indicated that the apoptosis level was significantly increased in SELENOK$^{-/-}$ (C13 and C15) N2a cells (Fig. 2A). M-calpain (calpain-2) has been reported to be responsible for the cleavage of procaspase-12 to produce active caspase-12 [23]. Cytosolic Ca^{2+} may increase activity of calpain enzymes, consistent with our results showing that the activity of calpain significantly increased in both in vitro (SELENOK$^{-/-}$ N2a cells) (Fig. 2I) and in vivo (the cortex and hippocampus of SELENOK$^{-/-}$ mice) (Fig. 2J). Therefore, we measured the expression levels of these enzymes and found that calpain-2, procaspase-12, active caspase-12, and active caspase-3 levels were significant elevated in SELENOK$^{-/-}$ (C13 and C15) N2a cells (Fig. 2B–C). Similarly, the levels of calpain-2, procaspase-12, active caspase-12, and active caspase-3 were also significantly increased in the cortex (Fig. 2D and E) and hippocampus (Fig. 2F and G) of SELENOK$^{-/-}$ mice.

Taken together, these data suggest that SELENOK deficiency promotes ERS-induced, caspase-12-dependent neuronal apoptosis both in vitro and in vivo.

3.4. ERS inhibitors reverses SELENOK deficiency-induced ERS and apoptosis in neurons

Cells were cultured with an ERS inhibitor (30 μM salubrinal or 100 μm 4-PBA) for 24 h, and then expressions of ERS and apoptosis marker proteins were assessed. We found that both 4-PBA and salubrinal treatment significantly reduced the expression levels of CHOP and cell apoptosis in SELENOK$^{-/-}$ (C13 and C15) N2a cells (Fig. 3A–E).

3.5. Calpain and ROS inhibitor treatment reverses SELENOK deficiency-induced apoptosis in neurons

Cells were exposed to Acetylcysteine (25 μM/mL), a well-known antioxidant, and then a significant reduction in ROS from SELENOK$^{-/-}$ (C13 and C15) N2a cells were observed (Fig. 4A). We also observed similar phenomena after cells were treated with a Calpain inhibitor Calpeptin, the activity Calpain also significantly reduced (Fig. 4C). These effects also lead to the decrease of apoptosis level in SELENOK$^{-/-}$ (C13 and C15) N2a cells (Fig. 4B. D).

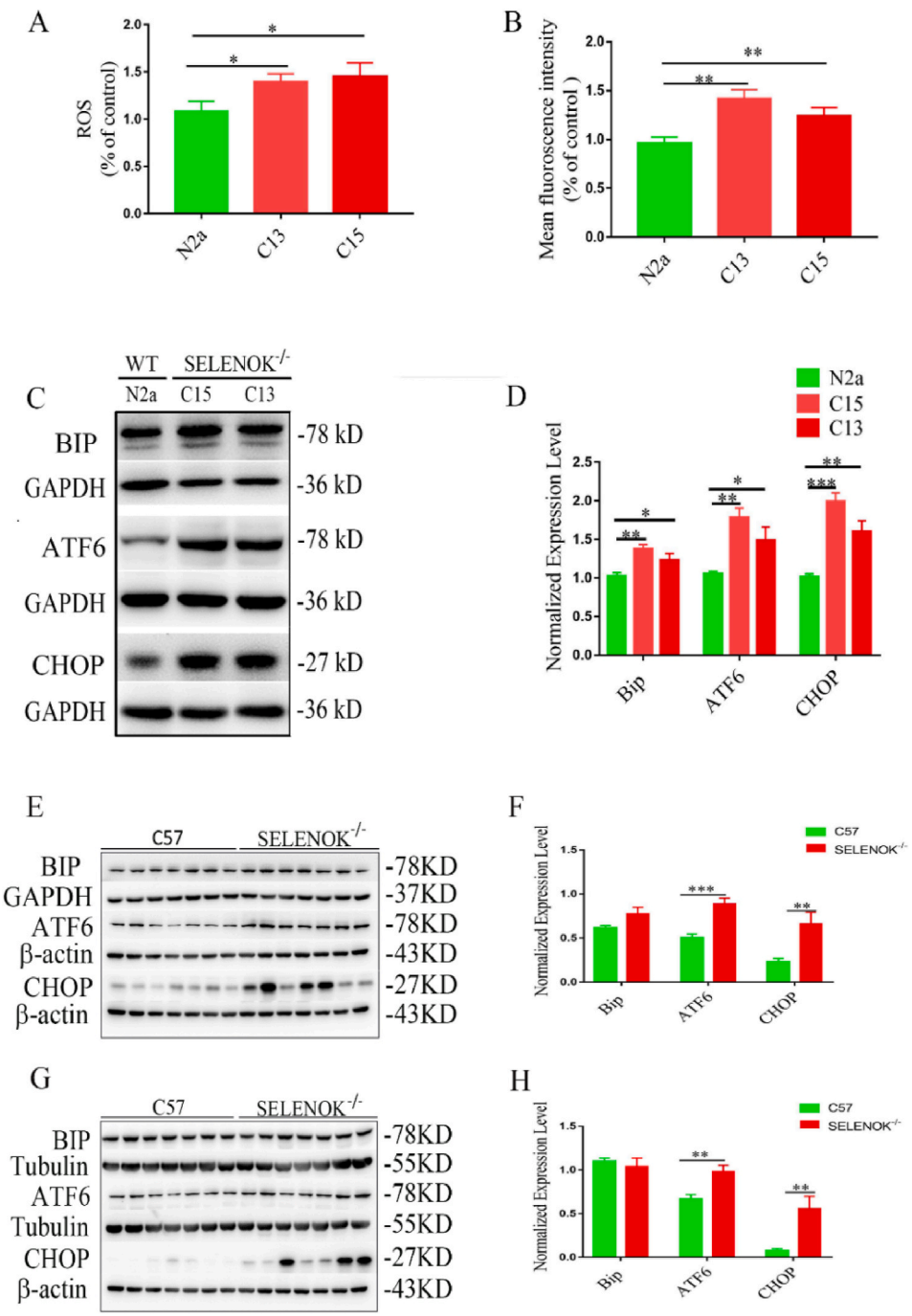

Fig. 1. SELENOK gene knockout induced increased ROS and ERS both in vitro and in vivo. (A) ROS levels were measured by flow cytometry after labeling with ROS assay kit (*$p < 0.01$ n = 3). (B) Intracellular Ca^{2+} levels were measured by flow cytometry after labeling with Fluo-3/AM. (**$p < 0.01$ n = 3). (C, D) Representative immunoblot analysis of BIP, ATF6, and CHOP in N2a cells and SELENOK$^{-/-}$ N2a cells (*$p < 0.05$, **$p < 0.01$, ***$p < 0.001$ n = 3).(E, F G, H) Representative immunoblot analysis of BIP, ATF6, and CHOP in cortical (E, F) and hippocampal (G, H) brain homogenates (*$p < 0.05$, **$p < 0.01$, ***$p < 0.001$ n = 7). The quantitative results were normalized to β-actin, GAPDH or α-tubulin expression.

3.6. Behavioral tests

Since the brain weight of SELENOK$^{-/-}$ mice was reduced, the cognitive ability of those mice was evaluated. Spatial learning was evaluated by determining the time required by the mice to find the hidden platform (i.e., escape latency) in the Morris water maze test. As shown in (Fig. 5A), there was no significant difference in escape latency between SELENOK$^{-/-}$ mice and WT controls. However, in the probe trials, the number of platform location crossings and time spent in the original platform quadrant were significantly decreased in SELENOK$^{-/-}$ mice compared to WT controls at 24 h and 72 h (Fig. 5B and C). No significant gender-related differences were found in Morris water maze test among SELENOK$^{-/-}$ mice (Figs. S3D–I).

In the fear conditioning test, we found that during the training period, SELENOK$^{-/-}$ mice exhibited a significantly longer freezing time than WT controls, indicating that SELENOK$^{-/-}$ mice were more fearful of strange environments (Fig. 5D). In the subsequent context test, there was no significant difference in freezing time between the two groups. However, the results of the altered context and conditional stimulus tests indicated that the freezing time of SELENOK$^{-/-}$ mice was significantly shorter than that of WT controls (Fig. 5D).

The anxiety level of the mice was evaluated by the open field test and elevated plus-maze test. In the elevated plus-maze test, the SELENOK$^{-/-}$ mice entered the open arm fewer times and spent less time in the open arm than the WT controls. However, the SELENOK$^{-/-}$ mice spent a significantly longer time in the closed arm than control mice (Fig. 6A and B). We found no significant differences between male and female SELENOK$^{-/-}$ mice in this test (Figs. S3A–C). The results of the open field

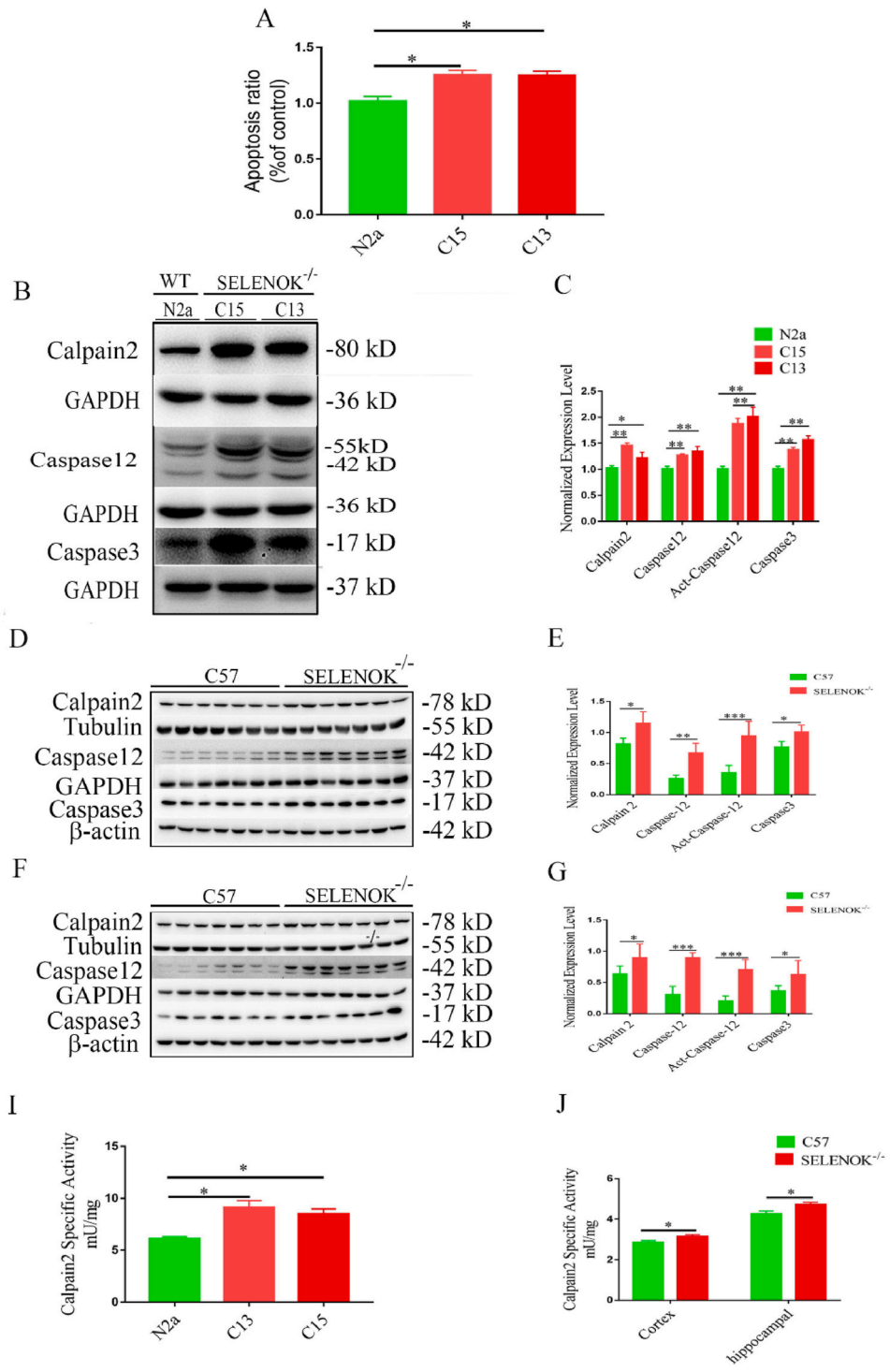

Fig. 2. SELENOK deficiency promoted ERS-induced neuronal apoptosis. (A) The effect of SELENOK gene knockout on apoptosis in the N2a cells, as determined by Annexin V-FITC labeling and flow cytometry analysis (*$p < 0.05$, n = 3). (B, C) Representative immunoblot analysis of calpain-2, caspase-12, active caspase-12, and active caspase-3 in WT and SELENOK$^{-/-}$ N2a cells (*$p < 0.05$, **$p < 0.01$, n = 3). (D, E, F, G) Representative immunoblot analysis of calpain-2, caspase-12, active caspase-12, and active caspase-3 in cortical (D, E) and hippocampal (F, G) brain homogenates (*$p < 0.05$, **$p < 0.01$, ***$p < 0.001$ n = 7). I, J) Calpain enzyme activity in N2a cells (I, *$p < 0.01$ n = 3), the cortical and hippocampal region of 7-months old mice (J, C57 n = 10, SELENOK$^{-/-}$ n = 9) were measured by ELISA(*$p < 0.05$). The quantitative results were normalized to β-actin, GAPDH or α-tubulin expression.

test showed that the number of rearing was no significant difference (Fig. 6C) but total distance traveled by the SELENOK$^{-/-}$ mice was shorter than that traveled by the WT controls (Fig. 6D). Altogether, these data suggest that SELENOK gene knockout in mice causes a significant decline in learning and memory abilities and increased anxiety.

4. Discussion

As an ER-resident selenoprotein, SELENOK has been reported to be mainly involved in regulating the redox equilibrium and modulating calcium flux. Overexpression of SELENOK in cultured cardiomyocytes decreases the level of intracellular ROS and protects cells from oxidative stress-induced toxicity. Reducing SELENOK levels in HepG2 cells impairs the antioxidant ability of the cells and significantly increases apoptosis after treatment with an ERS inducer such as TM [20,24]. In anti-CD3-stimulated SELENOK knockdown cells, the level of calcium homeostasis endoplasmic reticulum protein (CHERP) and the intracellular free Ca^{2+} concentration are significantly decreased [25]. SELENOK-deficiency also reduces Ca^{2+} flux in human melanoma cells [26]. Overexpression of SELENOK increases the cytosolic free Ca^{2+} level and induces apoptosis in human gastric cancer BGC-823 cells, but overexpression of SELENOK in HEK-293 cells does not cause a

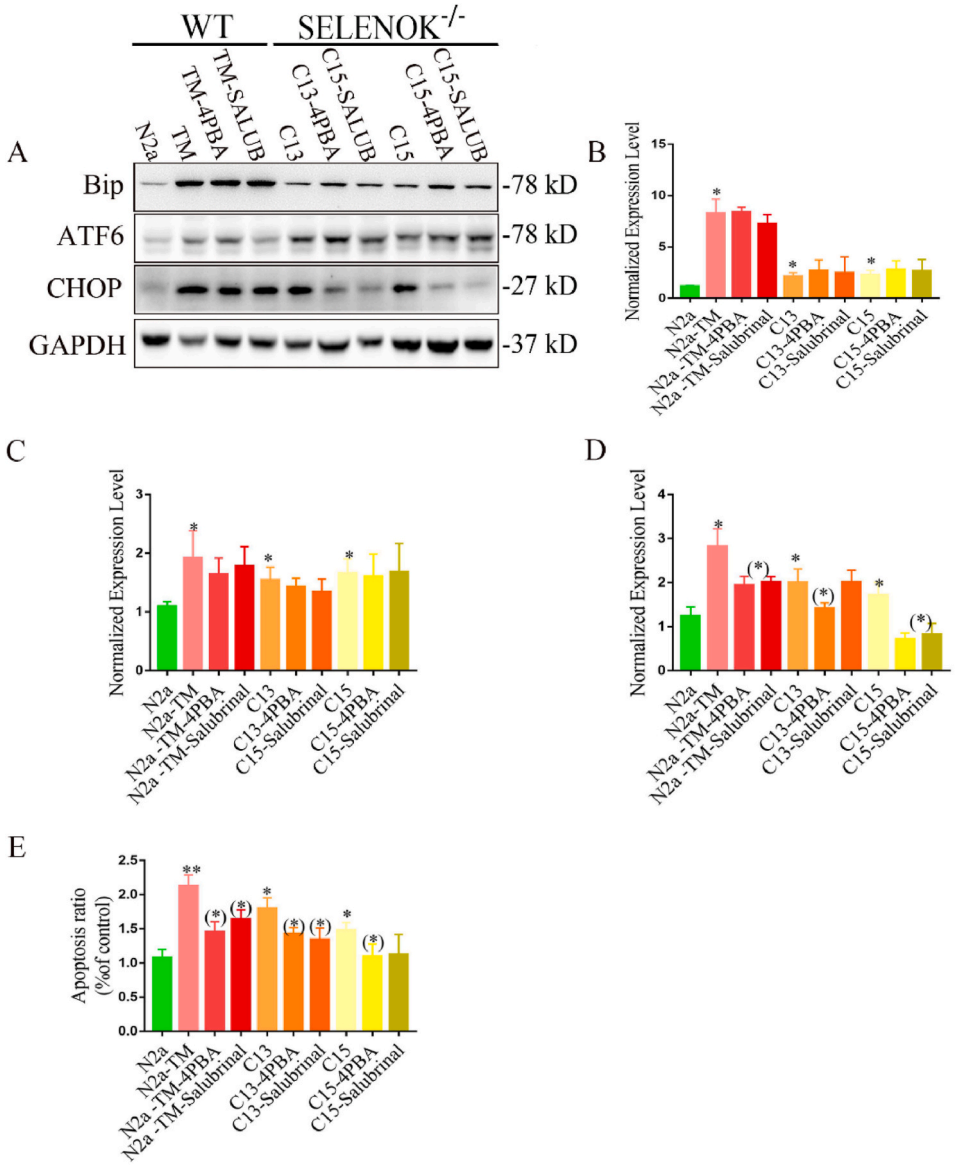

Fig. 3. ERS inhibitor treatment reverses the increase in CHOP expression and apoptosis in SELENOK$^{-/-}$ neurons. (A) Representative immunoblot analysis of BIP, ATF6, and CHOP expression in WT and SELENOK$^{-/-}$ N2a cells after treated with ERS inducer or inhibitors. Densitometric analysis of the levels of BIP (B), ATF6 (C), and CHOP (D). E) Apoptosis levels in WT and SELENOK$^{-/-}$ N2a cells treated by ERS inducer or inhibitors (*$p < 0.05$, versus N2a; (*) $p < 0.05$, versus C13 or C15 n = 3).

significant decrease in cell viability or apoptosis [27]. Herein, we demonstrated that SELENOK gene knockout markedly increased intracellular ROS and Ca^{2+} levels in N2a cells (Fig. 1A and B), suggesting that SELENOK also acts as an antioxidant and modulates Ca^{2+} levels in neurons. The ER is important for the folding, assembling, and post-translational modification of nascent proteins destined for secretion or insertion into the cell membrane. ER homeostasis can be disrupted through a variety of mechanisms including the accumulation of misfolded proteins [28], increased levels of ROS [29], and abnormal Ca^{2+} signaling [30]. All of these mechanisms contribute to ERS, which initiates the UPR involving three ERS sensor proteins: inositol-requiring kinase 1-alpha (IRE1α), PKR-like endoplasmic reticulum kinase (PERK), and ATF6. These proteins are negatively regulated by the chaperone GRP78 (BIP) under basal conditions [31,32]. Proteins that fail to fold properly within a certain period of time can activate the UPR and be subjected to ERAD. It has been shown that SELENOK is a component of the ERAD complex [33]. SELENOK has been reported to coprecipitate with soluble glycosylated ERAD substrates and participate in their degradation, and the SELENOK gene contains a functional ERS response element within its promoter region. SELENOK expression can be upregulated by the accumulation of misfolded proteins in the ER [11], suggesting that SELENOK is essential for maintaining ER homeostasis. In this study, we found that SELENOK gene knockout increased the levels of the ERS marker proteins BIP, CHOP, and ATF6 in N2a cells (Fig. 1C and D). Significant increases in CHOP and ATF6 levels were also observed in the cortices and hippocampi of SELENOK$^{-/-}$ mice (Fig. 1E–H), suggesting that loss of the SELENOK gene induces ERS in neurons.

In response to ERS, cells initiate protective responses to maintain homeostasis, but prolonged ERS also activates cell apoptosis signaling pathways [34]. Caspase-12 is a core player in ERS-induced apoptosis [35].

The release of stored Ca^{2+} from the ER can cause the activation of caspase-12, which can then activate caspase 3, leading to apoptosis [36]. Here, we found that in addition to elevating ERS marker levels, SELENOK gene knockout increased caspase-12 activity, suggesting that the

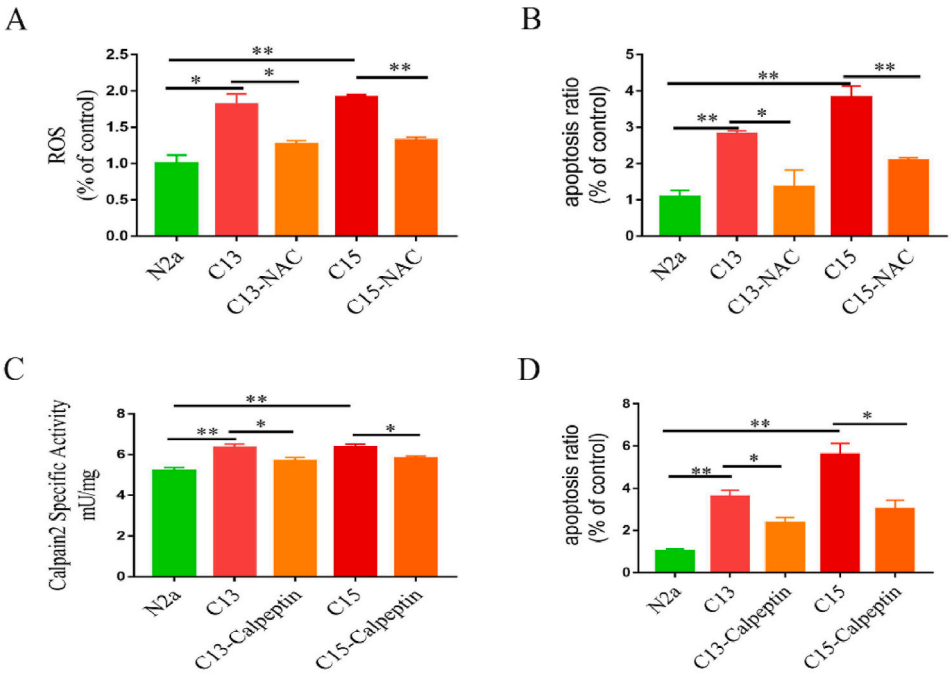

Fig. 4. Calpain inhibitor and ROS inhibitor treatment reverses apoptosis in SELENOK$^{-/-}$ neurons. (A) ROS levels were determined by a ROS assay kit and flow cytometry analysis. (*$p < 0.05$, **$p < 0.01$ n = 3). (C) Calpain enzyme activity was measured by ELISA (*$p < 0.05$, **$p < 0.01$ n = 5). (B, D) Apoptosis levels were tested by a Annexin V-FITC assay kit labeling and flow cytometry analysis. (*$p < 0.05$, **$p < 0.01$ n = 3).

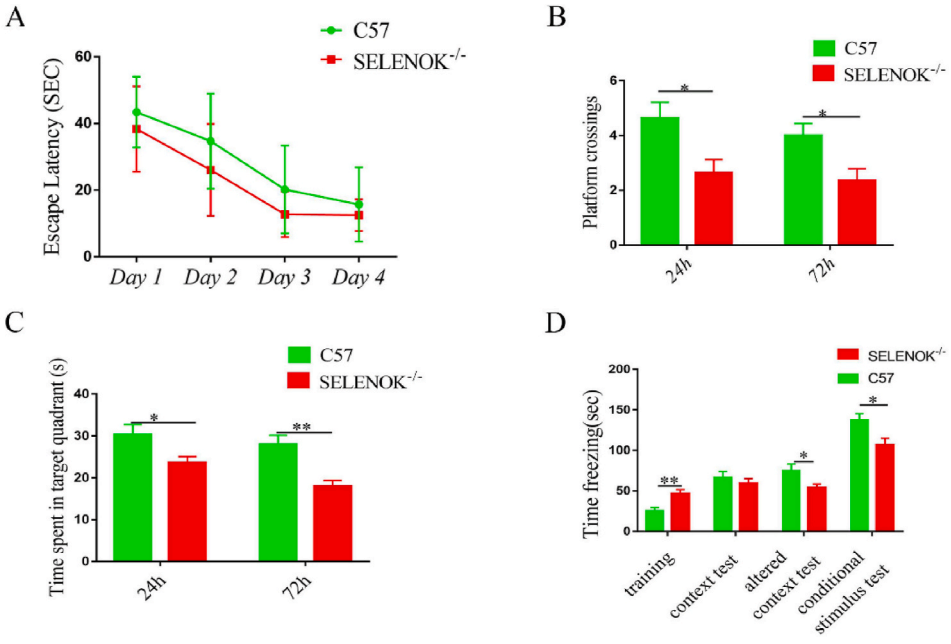

Fig. 5. Effect of SELENOK gene knockout in mice on spatial learning and memory, as determined by the Morris water maze test and fear conditioning test. (A) In hidden platform tests, mice were tested for 4 days and the escape latency of each mouse was recorded. (B, C) In the 24-h and 72-h probe trial, record the time that the mouse swims in the target quadrant where the hidden platform was previously placed and the number of times the mouse crosses the position of the platform (*$p < 0.05$). (D) Freezing time was observed for the SELENOK$^{-/-}$ mice compared to the WT controls in fear conditioning training, altered context test and conditional stimulus test. All numeric data are presented as the group mean ± SEM. A total of 17 mice were tested per group. *$p < 0.05$, **$p < 0.01$ versus the WT controls.

ERS-induced apoptotic pathway was activated (Fig. 2B–G). Studies have revealed that in vitro neuronal ischemia can lead to a parallel increase in Na^+ and Ca^{2+} levels in the cytoplasm, thereby activating caspase-12 [37]. Our observations are consistent with these views and suggest that the subsequent increase in the cytoplasmic Ca^{2+} level after SELENOK gene knockout leads to caspase-12 activation (Fig.1B; 2B-G). Procaspase-12 is predominantly localized in the ER and can be activated by ERS and calpain activity [22,38,39]. The expression level of calpain-2 was also significantly increased both in vitro and in vivo (Fig. 2B–G). We found that the calpain activity was significantly increased in SELENOK$^{-/-}$ (C13 and C15) N2a cells and SELENOK$^{-/-}$ mice brains (Fig. 2I and J). Calpain inhibitor (Calpeptin) significantly reduced calpain activity and apoptosis levels in SELENOK$^{-/-}$ (C13 and C15) N2a cells (Fig. 4C–D). Thus, SELENOK gene knockout might induce neuronal apoptosis by the Ca^{2+}-dependent calpain-caspase 12 pathway.

The data in this study indicate that SELENOK gene knockout can induce apoptosis through the ERS pathway. CHOP plays an important role in ERS-induced apoptosis [40]. During the initiation of the ERS pathway, CHOP can be induced by eIF2α and phosphorylated by PERK [41]. Here, we found that salubrinal, an inhibitor of eIF2α, reversed the increase in the CHOP expression level caused by SELENOK gene knockout (Fig. 3A–D). As a low molecular weight fatty acid, 4-PBA has

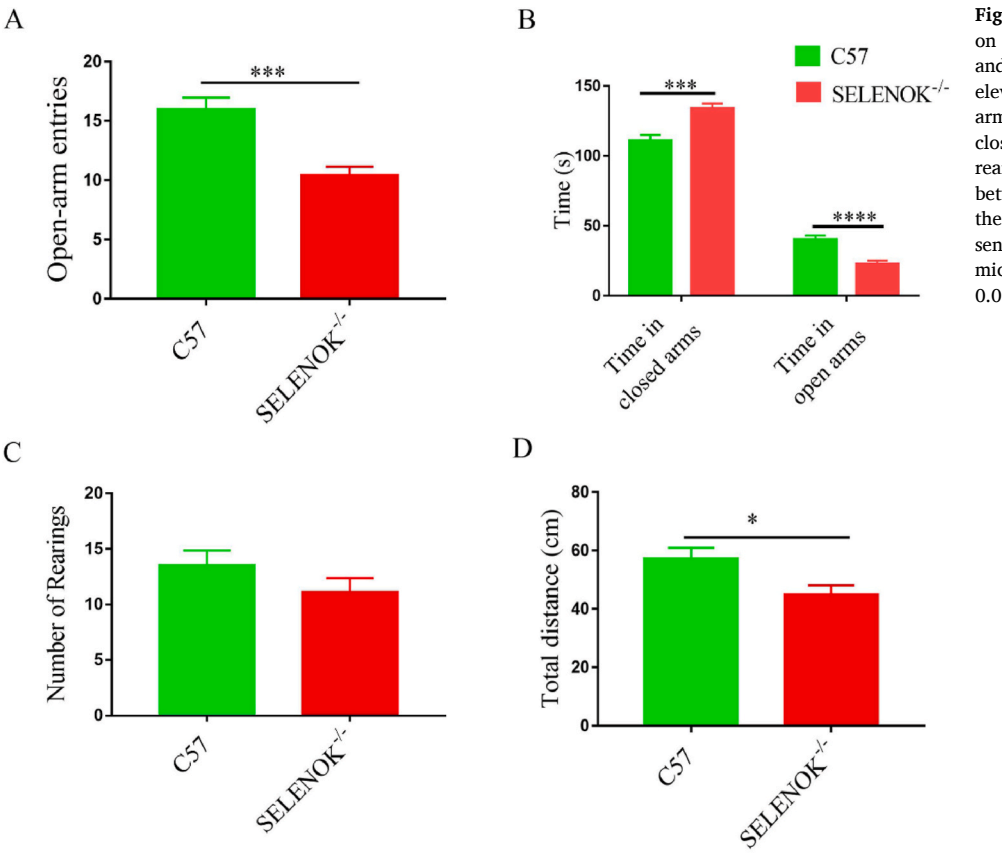

Fig. 6. Effect of SELENOK gene knockout in mice on anxiety, as determined by the open field test and elevated plus-maze test. (A, B) In the elevated plus-maze test, the times entered open arms, time in the open arms and time in the closed arms were showed. (C, D) Number of rearing and total distance traveled were observed between the SELENOK$^{-/-}$ and the WT controls in the open field test. All numeric data are presented as the group mean ± SEM. A total of 17 mice were tested per group. $*p < 0.05$, $**p < 0.01$, $***p < 0.001$ versus the control group.

been demonstrated to inhibit ERS [42,43]. Treatment with 4-PBA also reduced the increase in CHOP expression in neurons with SELENOK gene knockout (Fig. 3A–D). Increased ROS levels can disrupt endoplasmic reticulum homeostasis and cause ERS. In this study, we found that SELENOK gene knockout can increase the level of ROS (Fig. 1A). In addition, both ERS inhibitors and ROS inhibitors reduced cells apoptosis (Figs. 3E and 4B), providing further evidence to support the role of the ERS pathway in SELENOK gene knockout-induced apoptosis.

Here, we demonstrate that SELENOK gene knockout elevated intracellular Ca^{2+} levels and activated the calpain-mediated caspase-12-dependent apoptotic pathway in neurons both in vitro and in vivo. Neuronal apoptosis might further lead to cognitive impairments and anxiety in mice. The results of the behavioral tests suggested that SELENOK gene knockout caused a significant decline in memory and increased anxiety in mice (Fig. 5A–D; Fig. 6A–D). ERS pathway and calpain activation are associated with many neurodegenerative diseases including Alzheimer's disease (AD) [44–46]. AD is a neurodegenerative disease with neuropsychiatric symptoms such as anxiety and loss of memory [47,48]. Our previous study revealed that the expression level of SELENOK in 3xTg AD mice is significantly reduced [49]. Therefore, we speculate that SELENOK plays a major role in the regulation of ER homeostasis and exerts neuroprotective effects in vivo. Further study of the function of SELENOK will better reveal the important biological role of selenium and its underlying mechanism in the body.

Taken together, the data presented in this study establish a pathway of apoptosis initiated by SELENOK gene knockout (Fig. 7). The results demonstrate that SELENOK induces neuronal apoptosis through the ERS pathway. Specifically, SELENOK gene knockout initiates a series of cell death signaling events that are dependent on ERS, resulting in elevation of intracellular Ca^{2+} levels, activation of calpain and subsequent caspase-12-dependent apoptosis. Investigation into the mechanisms by which SELENOK exerts its effects in neurons may shed light on the mechanism of the effect of selenium in the brain and in AD.

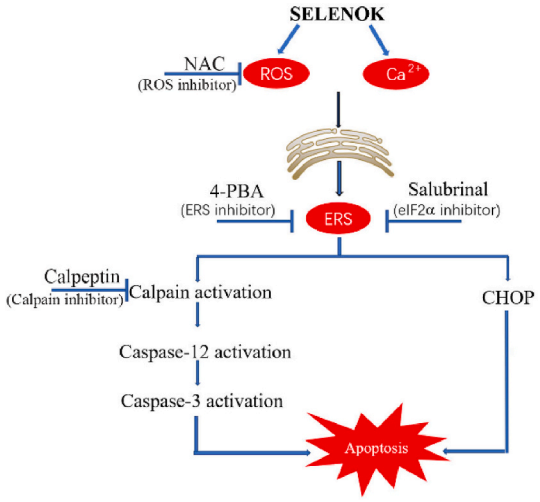

Fig. 7. Schematic model illustrating the mechanism of SELENOK gene knockout-induced apoptosis. SELENOK gene knockout increases intracellular Ca^{2+} and ROS levels. This activates the ERS pathway, as evidenced by induction of CHOP expression and activation of calpain. Calpain and CHOP activate caspase-12, which in turn activates caspase-3, leading to DNA fragmentation and apoptosis.

Declaration of competing interest

We declare that there is no conflict of interest in this work.

Acknowledgments

We thank Instrumental Analysis Center of Shenzhen University for

excellent technical assistance.

Appendix A. Supplementary data

Supplementary data to this article can be found online at https://doi.org/10.1016/j.redox.2021.102154.

References

[1] Y. Xu, Y. Li, H. Li, et al., Effects of Topography and Soil Properties on Soil Selenium Distribution and Bioavailability (Phosphate Extraction): A Case Study in Yongjia County, **China** Science of the Total Environment, 2018, pp. 240–248.

[2] J. Fang, P. Zhu, Z. Yang, et al., Selenium ameliorates AFB 1 induced excess apoptosis in chicken splenocytes through death receptor and endoplasmic reticulum pathways, Biol. Trace Elem. Res. (2018).

[3] Y.Z. Wang, X.A. Jia, J.Y. Zhao, et al., Effects of selenium deficiency on Ca transport function of sarcoplasmic reticulum and lipid peroxidation in rat, myocardium Biological Trace Element Research 36 (2) (1993) 159–166.

[4] F.K.W. Hoffmann, A.C. Hashimoto, L.A. Shafer, et al., Dietary selenium modulates activation and differentiation of CD4+ T cells in mice through a mechanism involving cellular free thiols, J. Nutr. 140 (6) (2010) 1155–1161.

[5] A. Nakayama, K.E. Hill, L.M. Austin, et al., All regions of mouse brain are dependent on selenoprotein P for maintenance of selenium, J. Nutr. 137 (3) (2007) 690–693.

[6] G.V. Kryukov, S. Castellano, S.V. Novoselov, et al., Characterization of mammalian selenoproteomes, Encephale 300 (5624) (2003) 1439–1443.

[7] J. Chen, M.J. Berry, Selenium and selenoproteins in the brain and brain diseases [J], J. Neurochem. 86 (1) (2003) 1–12.

[8] Verma, Saguna, Hoffmann, et al., Selenoprotein K knockout mice exhibit deficient calcium flux in immune cells and impaired immune responses, J. Immunol. 186 (4) (2011) 2127–2137.

[9] J. Liu, S. Rozovsky, Membrane-bound selenoproteins, 23, Antioxidants Redox Signal. 23 (10) (2015) 795–813.

[10] Y. Zhang, Y. Zhou, U. Schweizer, et al., Comparative analysis of selenocysteine machinery and selenoproteome gene expression in mouse brain identifies neurons as key functional sites of selenium in mammals, J. Biol. Chem. 283 (4) (2008) 2427–2438.

[11] V.A. Shchedrina, R.A. Everley, Y. Zhang, et al., Selenoprotein K binds multiprotein complexes and is involved in the regulation of endoplasmic reticulum homeostasis, J. Biol. Chem. 286 (50) (2011) 42937–42948.

[12] M.H. Smith, H.L. Ploegh, J.S. Weissman, Road to ruin: targeting proteins for degradation in the endoplasmic reticulum, Science 334 (6059) (2011) 1086–1090.

[13] Longquan, Yueqin Zuo, et al., PI3-kinase/Akt pathway-regulated membrane transportation of acid-sensing ion channel 1a/Calcium ion influx/endoplasmic reticulum stress activation on PDGF-induced HSC Activation, J. Cell Mol. Med. 23 (6) (2019) 3940–3950.

[14] Hoffmann, R. Peter, et al., Selenoprotein K and protein palmitoylation, Antioxidants Redox Signal. 23 (10) (2015) 854–862.

[15] G.J. Fredericks, F.K.W. Hoffmann, A.H. Rose, et al., Stable expression and function of the inositol 1,4,5-triphosphate receptor requires palmitoylation by a DHHC6/selenoprotein K complex, Proc. Natl. Acad. Sci. U. S. A 111 (46) (2014) 16478–16483.

[16] M. D'Eletto, F. Rossin, L. Occhigrossi, et al., Transglutaminase type 2 regulates ER-mitochondria contact sites by interacting with GRP75, Cell Rep. 25 (13) (2018) 3573–3581.

[17] V. Basso, E. Marchesan, E. Ziviani, A trio has turned into a quartet: DJ-1 interacts with the IP3R-Grp75-VDAC complex to control ER-mitochondria interaction, Cell Calcium 87 (2020) 102186.

[18] S. Verma, F.W. Hoffmann, M. Kumar, et al., Selenoprotein K knockout mice exhibit deficient calcium flux in immune cells and impaired immune responses, J. Immunol. 186 (4) (2011) 2127–2137.

[19] Z.H. Zhang, Q.Y. Wu, R. Zheng, et al., Selenomethionine mitigates cognitive decline by targeting both tau hyperphosphorylation and autophagic clearance in an Alzheimer's disease mouse model, J. Neurosci. 37 (9) (2017) 2449.

[20] S. DU, J. Zhou, Y. Jia, et al., SelK is a novel ER stress-regulated protein and protects HepG2 cells from ER stress agent-induced apoptosis, Arch. Biochem. Biophys. 502 (2) (2010) 137–143.

[21] W. Yao, X. Yang, J. Zhu, et al., IRE1α siRNA relieves endoplasmic reticulum stress-induced apoptosis and alleviates diabetic peripheral neuropathy in vivo and in vitro, Sci. Rep. 8 (1) (2018) 2579.

[22] T. Nakagawa, H. Zhu, N. Morishima, et al., Caspase-12 mediates endoplasmic-reticulum-specific apoptosis and cytotoxicity by amyloid-beta, Nature 403 (6765) (2000) 98–103.

[23] N.J. Yuan, Cross-talk between two cysteine protease families: activation of caspase-12 by calpain in apoptosis, JCB (J. Cell Biol.) 150 (4) (2000) 887–894.

[24] C. Lu, F. Qiu, H. Zhou, et al., Identification and characterization of selenoprotein K: an antioxidant in cardiomyocytes, FEBS Lett. 580 (22) (2006) 5189–5197.

[25] C. Wang, R. Li, Y. Huang, et al., Selenoprotein K modulate intracellular free Ca2+ by regulating expression of calcium homoeostasis endoplasmic reticulum protein, Biochem. Biophys. Res. Commun. 484 (4) (2017) 734–739.

[26] M.P. Marciel, V.S. Khadka, Y. Deng, et al., Selenoprotein K deficiency inhibits melanoma by reducing calcium flux required for tumor growth and metastasis, Oncotarget 9 (17) (2018) 13407–13422.

[27] S.B. Ben, B. Peng, G.C. Wang, et al., Overexpression of selenoprotein SelK in BGC-823 cells inhibits cell adhesion and migration, Biochemistry 80 (10) (2015) 1344–1353.

[28] P.E.T.E.R. Walter, Ron, et al., The unfolded protein response: from stress pathway to homeostatic regulation, Science 334 (6059) (2011) 1081–1086.

[29] M. John, Hourihan, E. Lorenza, et al., Cysteine sulfenylation directs IRE-1 to activate the SKN-1/Nrf2 antioxidant response, Mol. Cell 63 (4) (2016) 553–566.

[30] A.J. Ryan, J.L. Larson Casey, C. He, et al., Asbestos-induced disruption of calcium homeostasis induces endoplasmic reticulum stress in macrophages, J. Biol. Chem. 289 (48) (2014) 33391–33403.

[31] I. Tabas, D. Ron, Integrating the mechanisms of apoptosis induced by endoplasmic reticulum stress, Nat. Cell Biol. 13 (3) (2011) 184.

[32] B.M. Gardner, D. Pincus, K. Gotthardt, et al., Endoplasmic reticulum stress sensing in the unfolded protein response, Cold Spring Harbor Perspectives in Biology 5 (3) (2013) a013169.

[33] J.H. Lee, K.J. Park, J.K. Jang, et al., Selenoprotein S-dependent selenoprotein K binding to p97(VCP) protein is essential for endoplasmic reticulum-associated degradation, J. Biol. Chem. 290 (50) (2015) 29941–29952.

[34] S.L. Chan, W. Fu, P. Zhang, et al., Herp stabilizes neuronal Ca2+ homeostasis and mitochondrial function during endoplasmic reticulum stress, J. Biol. Chem. 279 (27) (2004) 28733.

[35] Q. Xie, Ribozyme-mediated inhibition of caspase-12 activity reduces apoptosis induced by endoplasmic reticulum stress in primary mouse hepatocytes, Int. J. Mol. Med. 22 (6) (2008) 717–724.

[36] B. Entaz, K. Hyongsuk, Y. Hyonok, ER stress-mediated signaling: action potential and Ca2+ as key players, Int. J. Mol. Sci. 17 (9) (2016) 1558.

[37] X. Chen, D.B. Kintner, J. Luo, et al., Endoplasmic reticulum Ca2+ dysregulation and endoplasmic reticulum stress following in vitro neuronal ischemia: role of Na+-K+-Cl- cotransporter, J. Neurochem. 106 (4) (2010) 563–576.

[38] Oshyuknakaawa, Honzhu, Nouhromorshma, et al., Caspase-12 mediates endoplasmic-reticulum-specific apoptosis and cytotoxicity by amyloid, Nature 403 (6765) (2000) 98–103.

[39] M. Shanmugam, A.E. Cribb, Calpain-induced endoplasmic reticulum stress and cell death following cytotoxic damage to renal cells, Toxicol. Sci. 1 (2006) 118–128.

[40] H. Hu, M. Tian, C. Ding, et al., The C/EBP homologous protein (CHOP) transcription factor functions in endoplasmic reticulum stress-induced apoptosis and microbial infection, Other 4 (9) (2018) 3083.

[41] C. Xu, B. Bailly-Maitre, J.C. Reed, C. Xu, B. Bailly-Maitre, J.C. Reed, Endoplasmic reticulum stress: cell life and death decisions. J Clin Invest 115: 2656-2664, J. Clin. Invest. 115 (10) (2005) 2656–2664.

[42] Z.S. Yue, L.R. Zeng, R.F. Quan, et al., 4Phenylbutyrate protects rat skin flaps against ischemiareperfusion injury and apoptosis by inhibiting endoplasmic reticulum stress, Mol. Med. Rep. 13 (2) (2016) pp1227–1233.

[43] S.R. Rao, S. Rajasekaran, S. Ajitkumar, et al., 4PBA strongly attenuates endoplasmic reticulum stress, fibrosis, and mitochondrial apoptosis markers in cyclosporine treated human gingival fibroblasts, J. Cell. Physiol. 233 (1) (2018) 60–66.

[44] C.Y. Wang, J.W. Xie, T. Wang, et al., Hypoxia-triggered m-calpain activation evokes endoplasmic reticulum stress and neuropathogenesis in a transgenic mouse model of Alzheimer's disease, CNS Neurosci. Ther. 19 (10) (2013) 820–833.

[45] Tetsumori Yamashima, Can 'calpain-cathepsin hypothesis' explain Alzheimer neuronal death? Ageing Res. Rev. 32 (2016) 169–179.

[46] Y.A.R. Mahaman, F. Huang, K.A. Henok, et al., Involvement of calpain in the neuropathogenesis of Alzheimer's disease, Med. Res. Rev. 39 (7) (2018).

[47] Y.U. Yun-Zhou, S.I. Liu, Hai-Chao Wang, et al., A novel aβ B-cell epitope vaccine (rCV01) for Alzheimer's disease improved synaptic and cognitive functions in 3 × tg-AD mice, J. Neuroimmune Pharmacol. 11 (4) (2016) 657–668.

[48] M. Johansson, E. Stomrud, O. Lindberg, et al., Apathy and anxiety are early markers of Alzheimer's disease, Neurobiol. Aging 85 (2019) 74–82.

[49] Z. Zhang, C. Chen, S. Jia, et al., Selenium Restores Synaptic Deficits by Modulating NMDA Receptors and Selenoprotein K in an Alzheimer's Disease Model, Antioxidants & Redox Signaling, 2020.